MICRO- AND MACRO-ANALYSIS OF THE FATIGUE CRACK GROWTH IN PEARLITIC STEELS

JESÚS TORIBIO, BEATRIZ GONZÁLEZ, JUAN-CARLOS MATOS

University of Salamanca, Department of Materials Engineering, E.P.S., Campus Viriato,
Avda. Requejo 33, 49022 Zamora, Spain.
toribio@usal.es

ABSTRACT: This paper deals with the influence of the manufacturing process on the fatigue behaviour of pearlitic steels with different degrees of cold drawing. The analysis is focussed on the region II (Paris) of the fatigue behaviour in which $da/dN=C(\Delta K)^m$, measuring the constants (C and m) for the different degrees of drawing. From the engineering point of view, the manufacturing process by cold drawing improves the fatigue behaviour of the steels, since the fatigue crack growth rate decreases as the strain hardening level in the material increases. In particular, the coefficient m (slope of the Paris laws) remains almost constant and independent of the drawing degree, whereas the constant C decreases as the drawing degree rises. The paper focuses on the relationship between the pearlitic microstructure of the steels (progressively oriented as a consequence of the manufacturing process by cold drawing) and the macroscopic fatigue behaviour. It is seen that the fatigue crack growth path presents certain roughness at the microscopic level, such a roughness being related to the pearlitic colony boundaries more than to the ferrite/cementite lamellae interfaces.

Keywords: Pearlitic Steel, High Strength Steel, Fatigue Microdamage, Paris' Law**.**

RESUMO: Este artigo trata da influencia do processo de fabricaçao no comportamento da fatiga de aços perliticos com graus diferentes de trefilado. A análise é centrada na região II (Paris) do comportamento da fatiga na que $da/dN=C(\Delta K)^m$, medindo as constantes (C e m) para os diferentes graus do proceso de fabricaçao. Desde o ponto da vista da engenharia, o processo de fabricaçao polo desenho en frio melhora o comportamento da fatiga dos aços, dende que a taxa de crescimento da fissura da fatiga diminui enquanto aumenta o nível de endurescemento por deformaçao do material. No detalhe, o coeficiente m (inclinação das leis de Paris) permanesce quase constante e independente do grau de trefilado, mentras que a constante C diminui enquanto o grau de trefilado se levanta. O artigo focalizase no relacionamento entre a microstructura perlitica dos aços (orientados progressivamente em consequência do processo de fabricaçao pelo desenho en frio) e o comportamento macroscópico da fatiga. Vê-se que o trajeto do crescimento da fissura da fatiga apresenta determinada aspereza no nível microscópico, tal aspereza está sendo relacionada aos limites da colônia perlítica mais do que puideran influir as intercaras das lamellas de ferrita/cementita.

Palavras chave: Aço Perlitico, Aço de alta ressistença, Microdano por Fatiga, Lei de Paris.

1. INTRODUCTION

Fatigue propagation is the basic subcritical mechanism of cracking. In pearlitic steel microstructures, the interlamellar spacing is the key parameter controlling fatigue crack growth, since the ferrite/cementite interfaces block the dislocation movement [1]. With regard to fatigue crack growth thresholds, they are strongly dependent on microstructure [2], in particular on the pearlitic colony size [3]. In addition, such a threshold decreases when the stress ratio (R factor) increases at constant temperature, such a decrease being higher at low temperatures [4]. In cold drawn pearlitic steel there is a linear inverse relationship between the stress ratio and the threshold, and the latter decreases when the yield strength increases [5].

In the matter of the Paris regime, although the role of microstructure is not clear for some authors [6], in cold drawn pearlitic steel the Paris' law shifts to lower values as the drawing degree increases, so that the fatigue crack growth resistance increases with cold drawing [7]. The presence of oriented pearlite promotes a tortuous crack path with local crack deflections and bifurcations [8,9], delaying fatigue crack growth due to the presence of the cementite hard phase.

2. EXPERIMENTAL PROCEDURE

The materials used were progressively drawn pearlitic steels with eutectoid chemical composition (0.789 % C, 0.681 % Mn, 0.210 % Si, 0.010 % P, 0.218 % Cr, 0.061 % V). Analysis covered from the hot rolled bar (steel E0 which is not cold drawn at all) to the cold drawn wire (commercial prestressing steel E7 suffering seven cold drawing steps), including the intermediate degrees of drawing too (steels E1 to E6, where the digit indicates the number of drawings steps undergone by each steel after passing through the successive drawing dies).

Pearlitic material microstructure consisted of alternate lamellae of ferrite and cementite whose orientation in relation to the wire axis depended on the drawing level [10-14]. As a summary of the effects of cold drawing on the evolution of the pearlite colony or first microstructural level [10,11], cold drawing produces a progressive orientation of the pearlite colony with its main axis approaching the axis of the wire or cold drawing direction, and a slenderizing of the colony itself. In the matter of the pearlitic lamellar microstructure or second microstructural level [12,13], cold drawing produces both a decrease of interlamellar spacing and an orientation of the plates in the cold drawing direction.

Apart from these general trends, the metallographic analysis showed the presence of some extremely slender pearlitic pseudocolonies with anomalous (too large) local inter-lamellar spacing and even with pre-damage (microcracks which act as local fracture precursors) which makes them preferential fracture paths with minimum local resistance [14].

The cold drawing process provokes an improvement of conventional mechanical properties of the steel. The yield strength and the ultimate tensile stress increase with cold drawing, whereas the Young's modulus keeps constant through the process. The stress-strain curves of the steels are plotted in Figure 1.

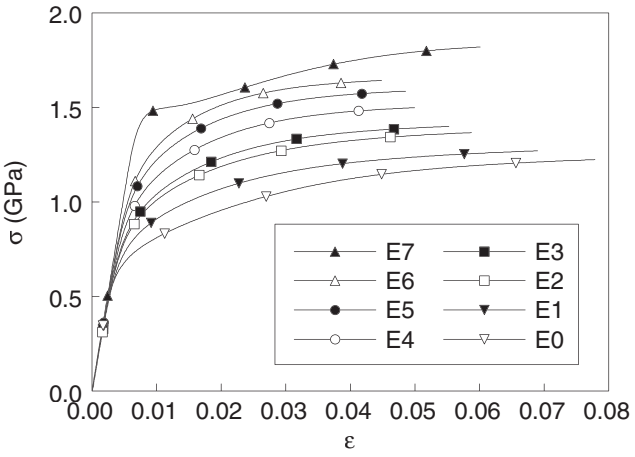

Fig. 1. Stress-strain curves of the steels.

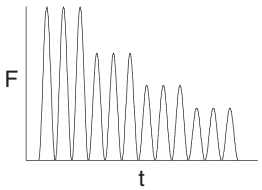

Fig. 2. Loading scheme during the tests.

The specimens for the fatigue tests were circular rods of 11.0 to 5.1 mm diameter and a mechanical notch was produced to initiate fatigue cracking. Tests were performed at room temperature, step by step under load control, the load being constant in a step and decreasing from one to another step. Samples were subjected to tensile cyclic loading with an R factor equal to zero, and a frequency of 10 Hz. The maximum load in the first loading stage corresponded to a value of about half the yield strength and was reduced between 20-30% from one to another step (Figure 2). Each loading stage was long enough to detect crack advance after the overload retardation effect [15] caused by the previous loading stage (with higher stress intensity level).

Fatigue test were interrupted and a fracto-metallographic analysis was performed on the cracked samples by cutting along a plane perpendicular to the crack front in order to exanimate in detail the fatigue crack path immersed in the steel microstructure. To this end, after grinding and polishing, samples were etched with 4% Nital during several seconds and later observed by scanning electron microscopy (SEM) with magnification factors of 3000x and 6000x.

3. EXPERIMENTAL RESULTS

3.1. Fatigue crack growth laws (hot rolled bar and prestressing steel wire)

The fatigue crack propagation was analyzed by using the Paris' law [16]:

$$\frac{da}{dN} = C\Delta K^m \tag{1}$$

by means of fatigue tests under load control, with constant stress range $\Delta\sigma$ during each step and decreasing steps (i.e., the stress range decreases from one to another step), where da/dN is the cyclic crack growth by fatigue and ΔK the stress intensity range, both variables being related by the equation:

$$\Delta K = Y\Delta\sigma\sqrt{\pi a} \tag{2}$$

The dimensionless stress intensity factor Y for the geometry under consideration (cracked wire) was calculated by Astiz [17] by means of the finite element method together with a virtual crack extension technique on the basis of the stiffness derivative, as a function of the relative crack depth (a/D) and the crack aspect ratio (a/b).

In the fractographs obtained by fatigue and posterior fracture of the wires, the crack front evolution was observed. The fatigue surfaces of the hot rolled bar and the cold drawn wire are developed in mode I and the beach marks being clearly detectable by visual inspection (Figure 3).

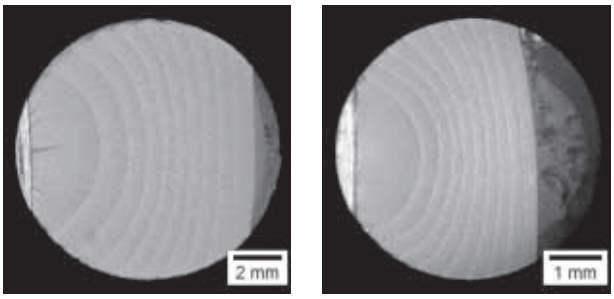

Fig. 3. Crack shape evolutions in steel wires E0 (hot rolled bar) and E7 (prestressing steel wire).

The crack front was modeled as an ellipse with its center located at the periphery of the rod. It was defined from a set of real points taken form the actual crack front and using a least squares fitting technique to adjust the theoretical (modeled) crack front to the real one.

The crack length was evaluated by means of the compliance of the samples, the dimensionless compliance ($1/CED$) versus the dimensionless crack length (a/D). The compliance (C) for each test was obtained from the last loading step at which the relationship between the applied load (F, measured by means of the load cell) and the relative displacement between two reference points in the sample (u, evaluated by means of a dynamic extensometer located in front of the crack mouth) allows the computation of the compliance $C=u/F$. Finally, the compliance was related to the crack geometry (relative crack depth a/D and crack aspect ratio a/b).

Figure 4 offers the fatigue crack growth curves (da/dN-ΔK) of both E0 and E7 in the Paris regime. From the engineering point of view, a clear improvement of fatigue performance is observed with cold drawing [18], the two lines being parallel, which indicates that the exponent of the Paris law is constant during the drawing process, whereas the constant C decreases with cold drawing (Table 1 where international units are used, i.e., when ΔK is used in $MPam^{1/2}$, da/dN appears in m/cycle). These results are consistent with previous analyses on progressively drawn steels [7].

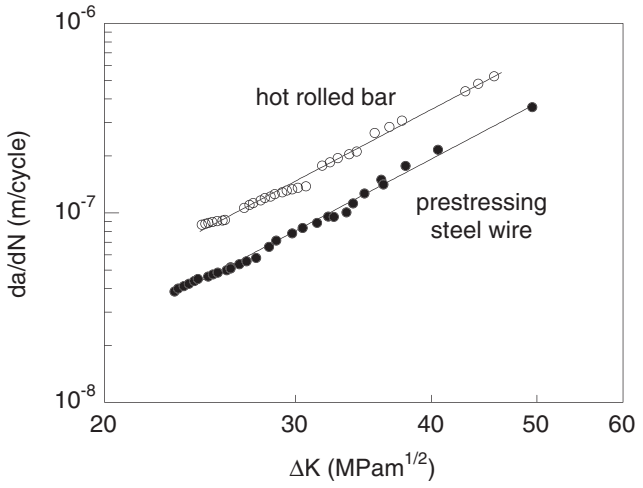

Fig. 4. Curves da/dN-ΔK of materials E0 (hot rolled bar) and E7 (prestressing steel wire).

Table 1. **Paris coefficients (S.I.).**

Steel	C	m
Hot rolled bar	$5.11 \cdot 10^{-12}$	3.02
Prestressing steel wire	$2.66 \cdot 10^{-12}$	3.03

3.2. Effect of residual stress (steels with intermediate degree of drawing)

Steels with intermediate degree of drawing exhibit a retardation of fatigue crack growth in the central area of the wire section (Figure 5) due to the presence of compressive residual stresses in that area and tensile ones in the vicinity of the wire surface. As a matter of fact, the cold drawing process generates an axisymmetric residual stress profile, so that such internal stresses affect the crack growth under cyclic loading, as discussed in [19]. Other analyses indicated that tensile residual stresses produce only a slight increase of crack propagation rate, while compressive ones create a big decrease [20]. As a consequence, residual stresses produces a gull-shaped crack front evolution in the central part of the cross-sectional area of the wires in the case of cold drawn steel, a phenomenon observed in other materials [21]. On the other hand, in the hot rolled steel (not cold drawn at all) and the commercial prestressing steel wire (which has undergone a stress-relieving process) the retardation effect (and its associated gull-shaped crack front) does not appear (cf. Figure 3).

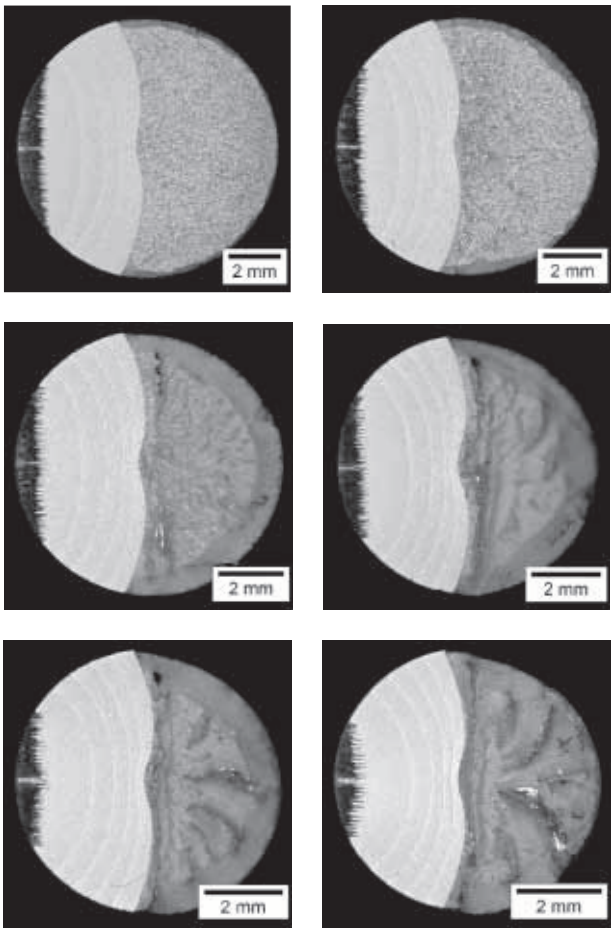

Fig. 5. Crack shape evolutions in intermediate steps (E1, E2, E3, E4, E5 and E6).

To quantify the afore-said phenomenon, a numerical modeling of the first step of cold drawing was perform by the finite element method using a commercial software (MSC Marc). The problem of a wire passing through a die has cylindrical symmetry, so that only an axial section of the cylinder has to be modeled (Figure 6). Cylindrical coordinates r, θ and z where used, z being the drawing axis, r the radial coordinate and θ the annular one. The finite element mesh was refined at wire axis and at the surface, the two zones where residual stress levels are higher. The stress-strain curve of the drawn steel used in

the computations was taken from the standard tension test (cf. Figure 1), whereas the die was considerated as rigid. The drawing process was modeled under displacement control. Large strains and large displacements were considerated in the computations.

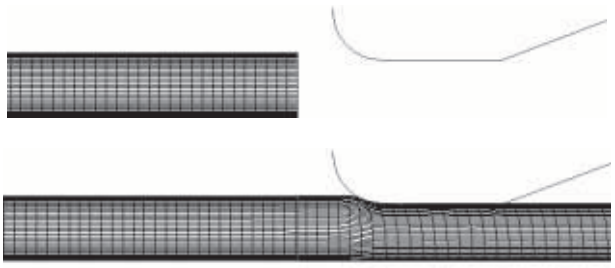

Fig. 6. Scheme of the drawing process.

Figure 7 shows the cylindrical components of residual stresses after one step of drawing. These distributions can be considered as representative of any degree of drawing in a real manufacturing process. Residual stresses are compressive at the wire center and tensile at the surface, the latter having higher absolute values, and this stress profile can explain the gull effect described above in the matter of crack shape evolution. With regard to the different components, radial, axial and annular stresses are in decreasing series.

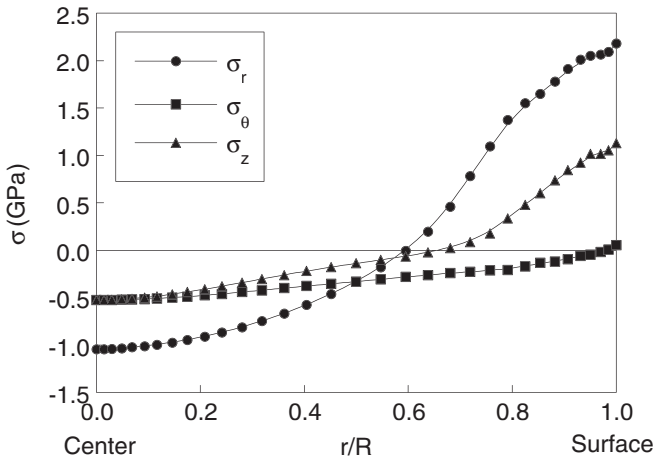

Fig. 7. Residual stresses in the drawn steel, where *r* is the radial coordinate and *R* the wire radius.

3.3. Microscopic approach: fatigue crack paths

To elucidate the microscopic crack path, metallographic sections were obtained from the fatigue cracked wires after cutting and polishing on a plane perpendicular to the crack front. Micrographs were taken showing the fatigue crack growth from left to right.

The fractographic appearance of fatigue cracks in pearlitic microstructures resembles microplastic tearing, consisted with fatigue damage and crack advance by highly localized plastic strain (Figure 8). Therefore the fatigue process could be caused by dislocational movement ending at the ferrite-cementite interfaces and promoting the fracture of pearlitic lamellae by plastic collapse. Fatigue cracks are transcolonial and tend to fracture pearlitic lamellae, with non-uniform crack opening displacement values, micro-discontinuities, branchings, bifurcations and local deflections, creating microstructural roughness (Figure 9).

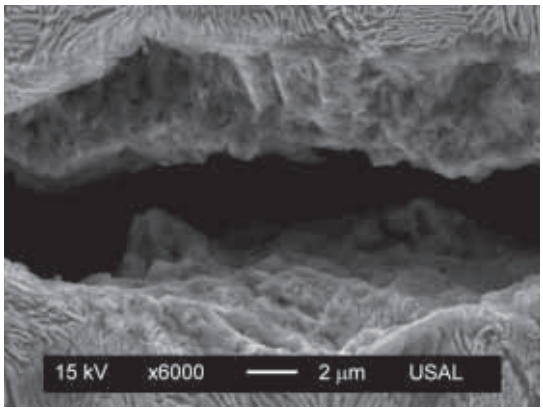

Fig. 8. Fracture surfaces.

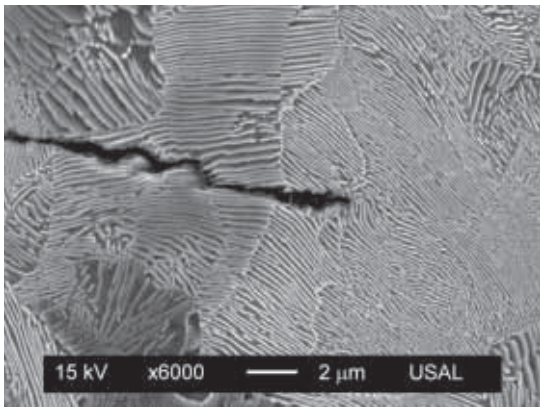

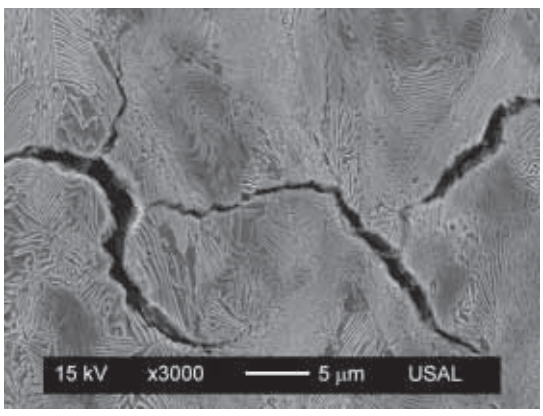

Fig. 9. Fatigue crack path in pearlitic steel (different drawing steps).

With regard to the role of the drawing degree, in Figures 10 and 11 the cracking profile is given in the hot rolled bar and the prestressing steel (cold drawn) wire for the same stress intensity range, showing that the frequency of deflections in the fatigue crack path increases with the cold drawing. This tortuous crack path is one of the basic explanations of the improvement of fatigue performance in the cold-drawn wire.

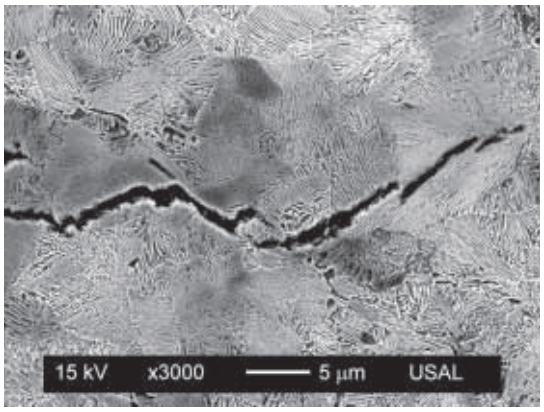

Fig. 10. Fatigue crack path (hot rolled bar).

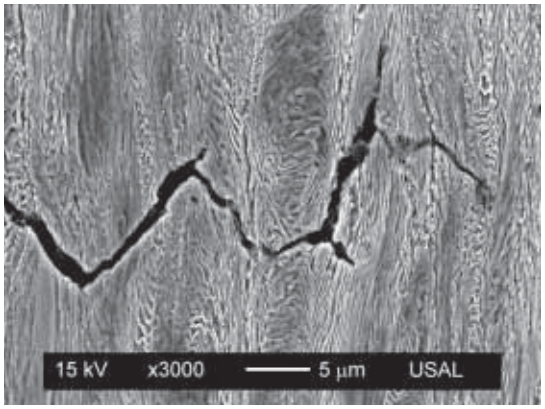

Fig. 11. Fatigue crack path (prestressing steel wire).

A computation was made of the ratio of the real profile length in the fatigue crack path, L_0, to the projected profile length, L (Figure 12). This ratio increases with cold drawing from 1.11 (hot rolled bar) to 1.23 (prestressing steel wire), thereby indicating that there is an increase of the net fatigue fractured surface with the degree of drawing, and the same happens with the frequency and angle of the local crack deflections in the fatigue crack path.

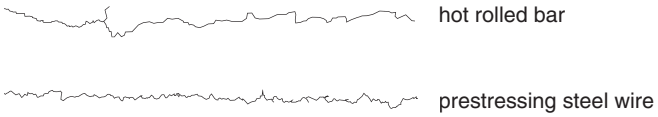

Fig. 12. Cracking profiles.

4. DISCUSSION

4.1. Global crack advance

To analyze the fatigue crack growth in both steels, metallographic cuts perpendicular to the fatigue crack path plane were made. It is seen that in both cases fatigue crack growth is through the pearlitic colonies (i.e., transcolonial), with higher roughness in the cold drawn wire and a growing direction changing from one to another colony. At the microscopic level, fatigue crack growth often exhibits some micro-crack branches with a deflection angle of about 45º in relation to the main crack growth direction (transverse to the wire axis). Such deflected branches could appear because fatigue cracking could follow a mechanism similar to that proposed by Miller and Smith [22] for static fracture in pearlitic microstructures. According to this mechanism of shear cracking in pearlite, brittle cementite lamellae fail when they are unable to undergo the big shear deformation of the more ductile ferrite.

This sub-section tries to analyze the key experimental result: the fact that the crack progresses in mode I by fatigue even in the cold drawn steel, in spite of its markedly oriented pearlitic microstructure and the presence of pearlitic pseudocolonies acting as local fracture precursors. The reasons for this behavior are three-fold:

(i) Crack tip blunting and large geometry changes produced by plasticity. As demonstrated in previous high-resolution numerical analyses by the finite element method [23], large strains and large geometry changes in the vicinity of the crack tip produce big rotations of axes and a clear crack tip blunting. Such a blunting is able to counterbalance the effect of the pearlitic pseudocolonies, so that posterior crack growth by fatigue in mode I after the crack has reached a pearlitic pseudocolony may be possible.

(ii) Geometrical constraint produced by the rest of the points of the crack front that therefore tends to propagate in the original direction. This fact makes the crack deflection by fatigue more difficult.

(iii) The orientation of the pearlitic lamellae. As a mater of fact, although in the cold drawn wire the plates are mainly oriented in the cold drawing direction and thus they are perpendicular to the crack faces, only some of them contain the crack front and tend to produce deflection, while many of them form and angle (or even are perpendicular) to the crack front, in the latter case tending to produce the more difficult phenomenon of crack twinning (two symmetrical branches).

4.2. Local crack advance

As commented above fatigue cracks are transcolonial and translamellar, tending to fracture the pearlitic lamellae. This is consistent with previous research on two-layer materials [24] in which an initial crack at the interface deviates to advance in one of the two constituents of the composite material, thus fracturing one of the layers. As a consequence of this phenomenon, fatigue crack paths are tortuous, with frequent local crack deflections and branchs, which confirms that a local mixed mode propagation takes place in the close vicinity of the crack tip under cyclic loading.

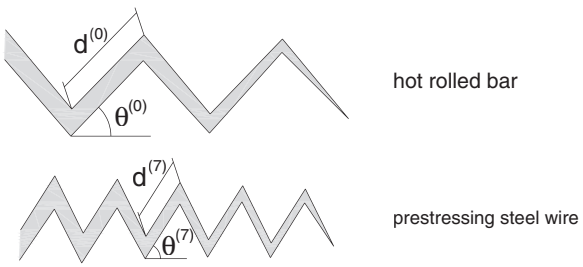

Fig. 13. Fatigue crack path scheme in both steels.

The decrease of pearlite interlamellar spacing with cold drawing [12] provokes a higher number of crack deflections in the fatigue crack path, while the drawing-induced microstructural orientation increases the angle of crack deflection.

Therefore, the prestressing steel wire exhibits a fatigue crack path containing more deflections than the hot rolled bar (Figure 13), the deflection path being shorter and the deflection angle being higher than in the former than in the latter, i.e.,

$$\theta^{(0)} < \theta^{(7)} \tag{3}$$

$$d^{(0)} > d^{(7)} \tag{4}$$

Some authors, e.g. [25] think that the fatigue crack propagation rate strongly depends on the orientation of the crack relative to the microstructure (either aligned or not), i.e., for cracks parallel to the aligned pearlitic lamellae the resistance of the microstructure against crack propagation is decreased while it is increased for cracks perpendicular to the alignment direction. However, our results contradict this idea, since the crack is able to propagate in the direction of apparently higher strength, i.e., breaking the pearlitic lamellae.

5. CONCLUSIONS

The cold drawing manufacturing process improves the fatigue performance of eutectoid steel by retarding the fatigue crack growth rate in the Paris regime, thus resulting that the manufacture process is beneficial from the points of view of damage tolerance and structural integrity of the prestressing steel wires.

Fatigue crack propagation in eutectoid steel wires under tensile loading in the Paris regime develops in mode I with an elliptical crack front. The crack is able to propagate by fatigue in mode I (with no crack deflection) even in the cold drawn steel, in spite of the markedly oriented pearlitic microstructure of the material in this case and the presence of pearlitic pseudocolonies (weakest regions). The reasons for this fact are the crack tip blunting and the large geometry changes produced by plasticity in the vicinity of the crack tip, the constraint produced by the rest of the points of the crack front and the different orientations of the pearlitic plates (in relation to the crack line) which would tend to produce crack twinning instead of crack deflection.

The steel wires with an intermediate cold drawing degree exhibit a retardation at the crack front center due to the presence of compressive residual stresses in the central area of the crack front (*gull effect*).

The fractographic appearance of the fatigue cracks resembles microplastic tearing, which is consistent with fatigue damage and crack advance by accumulation of plastic strain in the vicinity of the crack tip. From the microscopical point of view, the fatigue cracks are transcolonial and translamellar (i.e., the fatigue crack path crosses the colonies and breaks the lamellae). The crack opening displacement is not uniform along the crack, and many micro-discontinuities, branchings, bifurcations and local deflections appear, the latter especially in heavily drawn steels.

Thus the cold drawing process produces a tortuous crack path, so that the higher the cold drawing degree, the more tortuous the crack propagation path.

The key microstructural unit governing the fatigue crack growth is the pearlite arrangement (the key parameters being both the interlamellar spacing and the pearlitic plates orientation), since the ferrite-cementite interfaces block the dislocational movement, thereby producing a local retardation of the crack propagation and the afore-said tortuous crack path.

ACKNOWLEDGEMENTS

The authors wish to thank the financial support of their research at the University of Salamanca provided by the following institutions: Spanish Ministry for Education and Science (MEC; Grant BIA2005-08965), Regional Government Junta de Castilla y León (JCYL; Grants SA067A05 and SA111A07), Spanish Foundation "Memoria de D. Samuel Solórzano Barruso" (Grants for Scientific and Technological Research) and University of Salamanca (Grant USAL 2005-09). In addition, the authors wish to express their gratitude to Mr. Juan Monar (TREFILERÍAS QUIJANO, Cantabria, Spain) for providing the steel used in the experimental programme.

REFERENCES

[1] G.T. Gray III, A.W. Thompson and J.C. Williams, *Metall. Trans.* **16A** (1985) 753.

[2] S. Sankaran, V. Subramanya Sarma, K.A. Padmanabhan, G. Jaeger and A. Koethe, *Mater. Sci. Eng. A* **362** (2003) 249.

[3] K.S. Ravichandran, *Acta Metall. Mater.* **39** (1991) 1331.

[4] A.B. El-Shabasy and J.J. Lewandowski, *Int. J. Fatigue* **26** (2004) 305.

[5] J. Llorca and V. Sánchez-Gálvez, *Eng. Fracture Mech.* **26** (1987) 869.

[6] V. Subramanya Sarma, K.A. Padmanabhan, G. Jaeger, A. Koethe and M. Schaper, *Mater. Letters* **46** (2000) 185.

[7] J. Toribio and M. Toledano, *Proceedings of the "Seventh International Fatigue Congress"*, 1999, Beijing, China.

[8] A.A. Korda, Y. Mutoh, Y. Miyashita and T. Sadasue, *Mater. Sci. Eng. A* **428** (2006) 262.

[9] A.A. Korda, Y. Mutoh, Y. Miyashita, T. Sadasue and S.L. Mannan, *Scripta Mater.* **54** (2006) 1835.

[10] J. Toribio and E. Ovejero, *Mater. Sci. Eng. A* **234-236** (1997) 579.

[11] J. Toribio and E. Ovejero, *Mater. Sci. Lett.* **17** (1998) 1037.

[12] J. Toribio and E. Ovejero, *Scripta Mater.* **39** (1998) 323.

[13] J. Toribio and E. Ovejero, *Mech. Time-Dependent Mater.* **1** (1998) 307.

[14] J. Toribio, E. Ovejero and M. Toledano, *Int. J. Fracture* **87** (1997) L83.

[15] J. Toribio, B. González, J.C. Matos and F.J. Ayaso, *Key Eng. Mater.* **348-349** (2007) 681.

[16] P.C. Paris and F. Erdogan, *J. Basic Eng.* **85D** (1963) 528.

[17] M.A. Astiz, *Int. J. Fracture* **31** (1986) 105.

[18] J. Toribio, B. González and J.C. Matos, *Mater. Sci. Eng. A* **468-470** (2007) 267.

[19] A.K. Vasudevan, K. Sadananda and G. Glinka, *Int. J. Fatigue* **23** (2001) S39.

[20] M. Toyosada, T. Niwa and J. Sakai, *Int. J. Fatigue* **19** (1997) S161.

[21] C.Q. Cai and C.S. Shin, *Int. J. Fatigue* **27** (2005) 801.

[22] L.E. Miller and G.C. Smith, *J. Iron Steel Inst.* **208** (1970) 998.

[23] J. Toribio and V. Kharin, "Role of fatigue crack closure stresses in hydrogen assisted cracking", Advances in Fatigue Crack Closure Measurement and Analysis, PA, ASTM STP 1343, American Society for Testing and Materials, 1999.

[24] Y. Sugimura, L. Grondin and S. Suresh, *Scripta Metall. Mater.* **33** (1995) 2007.

[25] F. Wetscher, R. Stock and R. Pippan, *Mater. Sci. Eng. A* **445-446** (2007) 237.